

Systematic Analysis of the Phosphoproteome and Kinase-substrate Networks in the Mouse Testis*[§]

Lin Qi‡, Zexian Liu§, Jing Wang‡, Yiqiang Cui‡, Yueshuai Guo‡, Tao Zhou‡, Zuomin Zhou‡, Xuejiang Guo‡¶, Yu Xue§¶, and Jiahao Sha‡

Spermatogenesis is a complex process closely associated with the phosphorylation-orchestrated cell cycle. Elucidating the phosphorylation-based regulations should advance our understanding of the underlying molecular mechanisms. Here we present an integrative study of phosphorylation events in the testis. Large-scale phosphoproteome profiling in the adult mouse testis identified 17,829 phosphorylation sites in 3955 phosphoproteins. Although only approximately half of the phosphorylation sites enriched by IMAC were also captured by TiO₂, both the phosphoprotein data sets identified by the two methods significantly enriched the functional annotation of spermatogenesis. Thus, the phosphoproteome profiled in this study is a highly useful snapshot of the phosphorylation events in spermatogenesis. To further understand phosphoregulation in the testis, the site-specific kinase-substrate relations were computationally predicted for reconstructing kinase-substrate phosphorylation networks. A core sub-kinase-substrate phosphorylation networks among the spermatogenesis-related proteins was retrieved and analyzed to explore the phosphoregulation during spermatogenesis. Moreover, network-based analyses demonstrated that a number of protein kinases such as MAPKs, CDK2, and CDC2 with statistically more site-specific kinase-substrate relations might have significantly higher activities and play an essential role in spermatogenesis, and the predictions were consistent with previous studies on the regulatory roles of these kinases. In particular, the analyses proposed that the activities of POLO-like kinases (PLKs) might be dramatically higher, while the prediction was experimentally validated by detecting and comparing the phosphorylation levels of

pT210, an indicator of PLK1 activation, in testis and other tissues. Further experiments showed that the inhibition of POLO-like kinases decreases cell proliferation by inducing G2/M cell cycle arrest. Taken together, this systematic study provides a global landscape of phosphoregulation in the testis, and should prove to be of value in future studies of spermatogenesis. *Molecular & Cellular Proteomics* 13: 10.1074/mcp.M114.039073, 3626–3638, 2014.

Spermatogenesis is a complex sperm-generating process involving the mitosis of spermatogonia, meiosis of spermatocytes, and spermiogenesis of spermatids. Sperms are produced in the male testis at the speed of ~1000 sperm per heart beat (1), which indicate that spermatogenesis is an extremely dynamic process in the testis. The protein expression levels during spermatogenesis have been well studied by high-throughput proteomic studies, and over 7000 proteins have been identified in the mammalian testis (2–4). However, the dynamic regulatory events that orchestrate this complex process have yet to be elucidated. Because phosphorylation, an important and ubiquitous post-translational modification (PTM)¹, is one of the most critical regulatory mechanisms of the cell cycle (5), which is particularly active during spermatogenesis, a number of pioneering studies have contributed to our understanding of phosphoregulation in spermatogenesis. For example, mitogen-activated protein kinases (MAPKs) such as ERK1/2, were found to play an important role in ectoplasmic specialization dynamics during spermatogenesis (6). As important regulators of the cell cycle (7, 8), the POLO-like kinases (PLKs) especially PLK1, were found to be required at multiple stages of spermatogenesis (9–12). Thus, a systematic analysis of phosphorylation in the testis is of great

From the ‡State Key Laboratory of Reproductive Medicine, Department of Histology and Embryology, Nanjing Medical University, Nanjing, Jiangsu 210029, China; §Department of Biomedical Engineering, College of Life Science and Technology, Huazhong University of Science and Technology, Wuhan, Hubei 430074, China

Received, February 28, 2014 and in revised form, September 9, 2014

Published, MCP Papers in Press, October 7, 2014, DOI 10.1074/mcp.M114.039073

Author contributions: Z.Z., X.G., Y.X., and J.S. designed research; L.Q., Z.L., J.W., Y.C., and Y.G. performed research; L.Q., Z.L., T.Z., X.G., and Y.X. analyzed data; L.Q., Z.L., T.Z., X.G., and Y.X. wrote the paper.

¹ The abbreviations used are: PTM, post-translational modification; MAPK, Mitogen-activated protein kinase; PLK, POLO-like kinase; PFDoA, perfluorododecanoic acid; KSR, kinase-substrate relation; KSPN, kinase-substrate phosphorylation network; ssKSR, site-specific kinase-substrate relation; PPI, protein-protein interaction; KAA, kinase activity analysis; IMAC, immobilized metal affinity chromatography; TiO₂, titanium dioxide; GO, gene ontology; SCX, strong cation exchange; FDR, false discovery rate; LSD, least significant difference test; pS, phosphoserine; pT, phosphothreonine; pY, phosphotyrosine; FACS, fluorescence activated cell sorting; OA, okadaic acid.

importance for advancing the current understanding of the molecular mechanisms of spermatogenesis.

In order to elucidate the phosphorylation-mediated regulation of spermatogenesis, the characterization of the testicular phosphoproteome could serve as a straightforward start. Recently, rapid progress in mass spectrometry based proteomic technologies has greatly advanced to a state-of-art stage at which thousands of PTM sites can be identified in a single run (13). Although a large proportion of these studies were carried out in cell lines, only a handful of studies have contributed to the identification of phosphoproteome in testis and sperm (14–19). For example, Huttlin *et al.* identified ~36,000 phosphorylation sites in 6296 proteins from nine tissues, including the 3-week testis of immature mice (16). Because neither elongated spermatids nor sperms exist in such immature testes (16), it might be impossible to identify of phosphorylation sites across all stages of spermatogenesis from the samples. Moreover, a recent study characterized the testicular phosphoproteome in the perfluorododecanoic acid (PFDoA)-exposed rats, and demonstrated the importance of MAPK pathway and CDC2 protein phosphorylation in the toxicity of PFDoA (19). Taken together, despite the fact that a number of studies have been carried out (18), our understanding of the testicular phosphoproteome is still limited, and more effort needs to be expended on this area.

In coordination with the exploration of the phosphoproteome, the technology for analyzing kinase-substrate relations (KSRs) has also greatly advanced. In addition to conventional experimental approaches, a number of computational studies have been carried out (8, 20–23), whereas network approaches have attracted growing attention (20, 22). In 2007, Linding *et al.* first constructed a human kinase-substrate phosphorylation network (KSPN) through the prediction of site-specific kinase-substrate relations (ssKSRs) with a novel algorithm NetworkKIN (24, 25). Combined with sequence-based predictions using the Group-based Prediction System (GPS) algorithm and protein-protein interactions (PPIs), we also developed iGPS (*in vivo* GPS) software to reconstruct ssKSR-based KSPNs in eukaryotes, and achieved a superior performance compared with NetworkKIN (26). With these computational tools, network-based analyses can be performed for mining phospho-signatures from the phosphoproteomic data. For example, based on a hypothesis that a kinase with higher activity will phosphorylate more sites, we designed a novel computational method of kinase activity analysis (KAA) to statistically identify kinases with significantly more or less phosphorylation sites (20, 26). Using the human whole phosphoproteome as a background, we totally detected 60 kinases with higher activities (*i.e.* with more sites) from a human liver phosphoproteome (26). Our hypothesis and methodology was successfully supported by following studies, which used phospho-specific antibodies to validate the modification levels of the activity-associated autophosphorylation sites in the predicted kinases (27, 28). In particular, the two studies demon-

strated that kinases predicted with significantly higher activities can act as important regulators in distinct biological processes by regulating the KSPNs (27, 28). However, such an analysis of potentially differential kinase activities in spermatogenesis still remains to be performed.

In this study, we systematically profiled the phosphoproteome in the adult mouse testes. Using phosphopeptide enrichment methods, including immobilized metal affinity chromatography (IMAC) and Titanium dioxide (TiO₂), high-throughput mass spectrometry identified 17,829 phosphorylation sites in 3955 proteins in the adult mouse testis. Although only approximately half of the phosphorylation sites enriched by IMAC were also enriched by TiO₂, statistical analyses of the gene ontology (GO) terms consistently found the GO term “spermatogenesis” to be significantly over-represented. Thus, as the first comprehensive phosphoproteome in mature testis, these results provide an in-depth picture of phosphorylation in spermatogenesis. To further investigate phosphoregulation, the ssKSRs were predicted and employed to re-construct the KSPNs in the testis. Based on the working concept that kinases with a higher level of activity phosphorylate more sites (26), the predicted ssKSRs were used to predict the kinase activity profiles. Although the overlap of different phosphoproteome data sets is limited, the kinase activity profiles indicate a pattern of consistently high activity for a number of kinases, including the MAPKs, CDKs, and especially the POLO-like kinases (PLKs). Through Western blot detection of the phosphorylation levels of T210, which is positively correlated with PLK1 activation (29–32), it was observed that PLK1 was highly activated in testis. The PLKs inhibition assay results showed that PLKs activities are critical for cell proliferation in the spermatocyte GC2 cell line, whereas PLKs inhibition generated G2/M arrest. Taken together, this study of the testicular phosphoproteome provides a systematic understanding of the phosphorylation that occurs during spermatogenesis, with the results able to serve as a resource for future investigation.

EXPERIMENTAL PROCEDURES

Sample Preparation—For each replicate, six testes from three adult C57BL/6 mice were decapsulated and lysed in RIPA lysis buffer (25 mM Tris-base, 150 mM NaCl, 1% Sodium deoxycholate, and 1% SDS, and pH = 7.6) with a mixture of phosphatase inhibitors (200 mM Na₃VO₄ and 200 mM NaF), or urea lysis buffer (8 M urea, 75 mM NaCl, 50 mM Tris, pH 8.2, 1% mixture, 1 mM NaF, 1 mM β-glycerophosphate, 1 mM sodium orthovanadate, and 10 mM sodium pyrophosphate). The lysates were sonicated for 3s and cooled in ice to avoid overheating. This procedure was repeated three times and then followed by centrifugation at 40,000 × *g* for 60 min (4 °C). In total, 20–25 mg proteins were harvested for each replicate. All experiments requiring animals received prior approval from Nanjing Medical University and were performed according to United States Department of Agriculture-approved protocols.

Proteolytic Digestion—The proteins in RIPA lysis buffer were reduced at 56 °C for 60 min in DTT and subsequently alkylated in the dark with iodoacetamide at room temperature for 45 min. A sixfold volume of acetone precipitating solution was added overnight at

–20 °C. The next day, the supernatant was discarded after centrifugation at $8000 \times g$ for 10 min (4 °C). For subsequent digestion with trypsin, the solution was diluted with 25 mM ammonium bicarbonate (pH 8.5). Trypsin was added (1:50, w/w) and digestion was carried out overnight at 37 °C and subsequently quenched by the addition of TFA to a final concentration of 0.5% (34).

The proteins in urea lysis buffer were reduced by DTT and alkylated with iodoacetamide. The protein mixture was diluted (1:5) in 25 mM Tris-HCl, pH 8.2, to reduce the concentration of urea to 1.6 M. The proteins were then digested by trypsin at 37 °C overnight and subsequently quenched by the addition of TFA.

Strong Cation Exchange (SCX) Fractionation—The digested peptides were desalted by reverse-phase tC18 SepPak solid-phase extraction cartridges from the Waters Co. (Milford, MA), and subjected to SCX fractionation. SCX fractionation was performed on a 9.4×200 mm column packed with polysulfoethyl aspartamide material (5 μ m, 200 Å) at a flow rate of 3 ml/min using 5 mg peptides in each experiment. For fractionation, buffer A (7 mM KH_2PO_4 /30% CH_3CN /pH 2.65) and buffer B (7 mM KH_2PO_4 , 350 mM KCl, pH 2.65, and 30% ACN) were employed under a 40 min gradient (0% to 25% buffer B for 33 min, 25% to 100% buffer B for 1 min, 100% buffer B for 5 min, and 100% to 0% buffer B for 1 min). The separated peptides were collected for each 4-min period and finally 12 fractions were collected. Each fraction was desalted using a Waters SepPak column.

Phosphopeptide Enrichment by TiO_2 — TiO_2 beads (GL Sciences, Tokyo, Japan) were mixed at a ratio of 1:4 (Peptides:Beads) and then preincubated in 500 μ l loading buffer (65% ACN/2% TFA/saturated by glutamic acid) for acidification. The peptide samples were resolved in 200 μ l loading buffer and then incubated with the TiO_2 beads. For consecutive incubations, the peptide-beads slurry was incubated and centrifuged, and then the supernatant was incubated with another aliquot of freshly prepared TiO_2 beads for the next enrichment. The incubated beads were then washed with 800 μ l wash buffer I (65% ACN/0.5% TFA) and wash buffer II (65% ACN/0.1% TFA). The bound peptides were eluted once with the 200 μ l elution buffer I (300 mM NH_4OH /50% ACN) and twice with 200 μ l elution buffer II (500 mM NH_4OH /60% ACN). All the incubation, washing and elution procedures were rotated end-over-end for 15 min at room temperature (35). The eluates were dried and then purified on C18 StageTips (36), followed by the identification using mass spectrometry. The sample preparing, digestion, fractionation, TiO_2 -based enrichment, and following identification was replicated triply.

Phosphopeptide Enrichment by IMAC—IMAC beads were prepared by washing them with 1 ml of IMAC binding buffer (40% ACN (v/v) and 25 mM FA in H_2O). The vial was turned over a few times to resuspend all of the beads and spun to remove the liquid. This was repeated three times and a 50% slurry prepared in the same buffer. Each desalting peptide was dissolved in 120 μ l of IMAC-binding buffer and transferred to 10 μ l of prepared IMAC beads. Peptides were incubated on beads for 60 min, with vigorous shaking at room temperature. The resin was washed with 120 μ l of IMAC binding buffer. This step was repeated twice. Phosphopeptides were eluted by incubating them for 15 min with 40 μ l of IMAC elution buffer A (50 mM K_2HPO_4 / NH_4OH , pH 10.0). This step was repeated twice. Eluates from the same sample were combined in the same tube, neutralized with 40 μ l of 10% FA and dried by vacuum centrifugation at room temperature for subsequent identification. The sample preparing, digestion, fractionation, IMAC-based enrichment, and following identification was replicated twice.

MS Acquisition—The enriched phosphopeptides were analyzed using LTQ Orbitrap Velos (ThermoFinnigan, San Jose, CA) coupled directly to an LC column. The trap column effluent was transferred to a reverse-phase microcapillary column (0.075×150 mm, Acclaim®

PepMap100 C18 column, 3 μ m, 100 Å; DIONEX, Sunnyvale, CA). Reverse-phase separation of the peptides was performed using 2% ACN, 0.5% acetic acid (buffer A), and 80% ACN, 0.5% acetic acid (buffer B) under a 238 min gradient (4% to 30% buffer B for 208 min, 30% to 45% buffer B for 20 min, 45% to 100% buffer B for 1 min, 100% buffer B for 8 min, and 100% to 4% buffer B for 1 min). An MS survey scan was obtained for the m/z range 350–1800, and MS/MS spectra acquired in LTQ from the survey scan for the 20 most intense ions (determined using Xcalibur mass spectrometer software in real time). Dynamic mass exclusion windows of 60 s were used, with siloxane (m/z 445.120025) as the lock mass.

Database Search—Raw files were processed using MaxQuant version 1.3.0.5 (37) with default settings and searched against the UniProt mouse protein database (UniProt 2013_11; 43,236 sequences) combined with the standard MaxQuant contaminants database (38). Enzyme specificity was set as full cleavage by trypsin, with two maximum missed cleavage sites permitted. The minimum peptide length required was six and Carbamidomethyl (C) was set as a fixed modification. The variable modifications included oxidation (M), acetylation (Protein N-term) and phosphorylation (STY). The mass tolerance for the precursor ions and fragment ions was set to 20 ppm and 0.5 Da, respectively.

The false discovery rate (FDR) was estimated by searching against the databases with the reversed amino acid sequences. The site, peptide and protein FDR were set to 0.01. The minimum Maxquant score for phosphorylation sites was 30. We also constructed an online database called the “Phosphoproteome of mouse testis” to enable sharing of the results. The database is freely available at <http://reprod.njmu.edu.cn/phosmt/>. It provides detailed information on the identified phosphorylation sites, including modified amino acid, site probabilities, sequence window, mass, charge, representative annotated best spectra, the UniProt protein entry, and gene name. The mass spectrometry proteomics data including the annotated mass spectra have been deposited to the ProteomeXchange Consortium (<http://proteomecentral.proteomexchange.org>) via the PRIDE partner repository (39) with the data set identifier PXD000767.

Bioinformatic Analyses of Testis Phosphoproteome—Previously, Huttlin *et al.* identified the phosphoproteome in nine mouse tissues including the testis (16). The phosphopeptides were retrieved and remapped with the mouse proteome (UniProt 2013_11) (38), and in total 36,945 phosphorylation sites in 7259 proteins (designated as “Atlas”) were obtained, whereas 11,713 phosphorylation sites in 3087 proteins (designated as “Gygi’s”) were obtained from the testis. The phosphoproteome enriched by IMAC and TiO_2 in this study were designated as “IMAC” and “ TiO_2 ,” respectively, whereas the entire phosphoproteome profiled in this study was designated as “Total.” The GO annotations were retrieved from mouse gene association file, which was downloaded from the QuickGO database (40). As previously described (8), we statistically analyzed the enrichment of the GO terms in the data sets against the mouse proteome with a hypergeometric distribution (p value $< 10^{-5}$). The GO heatmaps were visualized by the ggplot2 program (<http://had.co.nz/ggplot2/>) in the R package (<http://www.r-project.org/>).

Using the iGPS software package (<http://igps.biocuckoo.org>) previously developed in-house (26), we systematically predicted potential ssKSRs for the five data sets (*i.e.* The Benchmark, Gygi’s, IMAC, TiO_2 , and Total data sets), using the default threshold (Low threshold, Experimental/String PPI filter). The predicted ssKSRs were employed to construct the KSPNs, whereas all of the networks were visualized with Cytoscape (version 2.8.2) (41). Again, based on the hypothesis that kinases with higher activities may phosphorylate more sites (26), the number of ssKSRs for a kinase were used as number representing the activity of the kinase. To find data set-specific high-activity ki-

TABLE I
Primers used in this study

Gene	Forward primers (5'- . . . -3')	Reverse primers (5'- . . . -3')	Amplicon size (bp)
PLK1	TTCCCAAGCACATCAACCCA	GCTGGGAGCGATTGAAAACC	182
PLK2	TTCTGCAGGGTTTCACTCC	GCTGCTGGGTATCGACACT	232
PLK3	GTGGCCACAGTGGTAGAGTC	GCACCGTCTTCCTATTGGCT	235
β -actin	CCGTAAAGACCTCTATGCC	CTCAGTAACAGTCCGCCTA	278

nases, the KAA approach was adopted and the kinase activity computed for the Atlas data set was employed as the control. Yates' Chi-square test was used to detect high-activity kinases for the Gygi's, IMAC, TiO₂, and Total data sets (*p* value < 0.05). The heatmaps for kinase activity were also visualized using the ggplot2.

Western Blot Analysis of the Expression and Phosphorylation of PLK1—The tissues from adult C57BL/6 mice were decapsulated and lysed in urea lysis buffer as above, and the lysates were sonicated followed by centrifugation at 14,000 rpm for 40 min (4 °C). Protein concentrations were determined by Bradford assay. 20 μ g proteins were loaded per lane to SDS-PAGE, and then transferred to nitrocellulose membranes. The membranes were blocked 1h in 5% milk at room temperature and incubated overnight at 4 °C with primary mouse anti-PLK1, rabbit anti-PLK1 (phospho T210), or mouse anti- β actin antibody (Abcam, Cambridge, UK), and the membranes were washed in TBST, and incubated for 1h with HRP conjugated goat anti-rabbit IgG(H+L) (1:2000, Thermo Fisher Scientific Inc., Rockford, IL) or goat anti-mouse IgG(H+L) (Thermo Fisher Scientific Inc.) at room temperature and washed again. Specific proteins were detected using an ECL kit and Alphascreen (GE Healthcare Bio-Sciences Corp., Piscataway, NJ).

RNA Extraction, RT-PCR—Total RNA was extracted from a GC2 cell line using the RNeasy Plus Micro Kit with oncolumn DNase digestion (Qiagen Ltd., Crawley, West Sussex, UK). Randomly primed cDNA was prepared using the Prime-Script™ RT Master Mix (TaKaRa Bio Inc., Otsu, Japan). The primer sequences used are shown in the Table I. The cDNAs were PCR-amplified with specific primers in 20 μ l of GoTaq Green Master Mix (Promega Corporation, CA, USA). The amplification conditions consisted of an initial denaturation at 94 °C for 5 min, followed by 30 cycles at 94 °C for 30 s, 55 °C for 30 s, and 72 °C for 30 s. The final extension was carried out at 72 °C for 10 min. The PCR products were analyzed with 2% w/v agarose gel electrophoresis using mouse β -actin as the control gene.

Culture of GC2 Cells—Mouse GC2 cells (ATCC catalog number CRL-2196, Manassas, VA, USA) were cultured for 16 h at 37 °C in 5% CO₂ in DMEM culture medium supplemented with 10% fetal bovine serum, 0.5% penicillin and streptomycin. For the inhibition assay, GC2 cells were treated with 100 nM BI 2536 (Selleck Chemicals LLC, Houston, TX) diluted in DMSO and controls were treated with DMSO alone. To inhibit phosphatases, GC2 cells were treated with 1 μ M OA (Millipore Corp., Billerica, MA) diluted in DMSO and controls were treated with DMSO alone. The time course experiment was carried out by treatment with 100 nM of BI 2536 for 2h, 4h, and 6h, with or without 1 μ M OA. GC2 cells were washed twice with PBS, digested with 0.25% trypsin, then harvested and fixed by 75% Ethanol overnight. GC2 cells was stained with PI (BD Biosciences, San Diego, CA) and analyzed with a BD FACS Calibur flow cytometry system (BD Biosciences). The statistical comparisons were performed by one-way ANOVA, and Least Significant Difference Test (LSD) was used for pair-wise comparisons if the variances were equal. A *p* value less than 0.05 was considered significant. The data are presented as the mean \pm S.E.

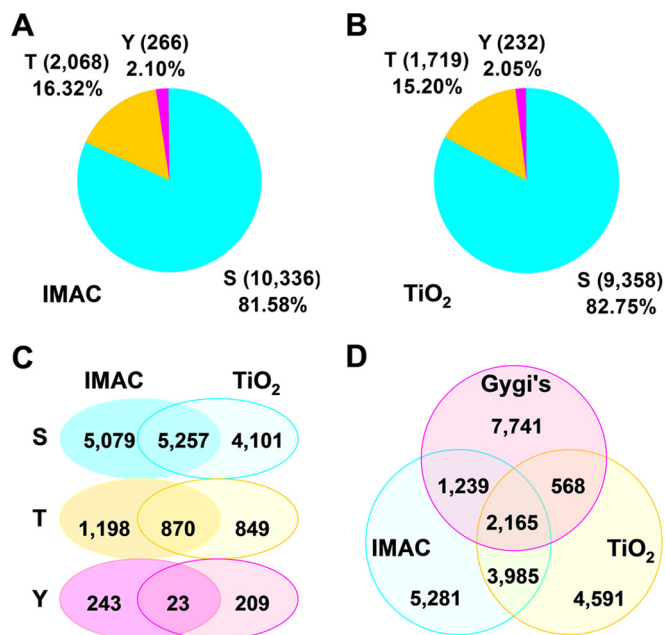


FIG. 1. Summarization of the phosphorylation sites identified in this study. A, The distribution of different residue types (S/T/Y) for the phosphorylation sites identified by IMAC or TiO₂. B, in this study. C, Summarization of the overlap of the phosphorylation sites identified by IMAC or TiO₂ for different residue types. D, Summarization of the overlap of the phosphorylation sites identified by IMAC and TiO₂ in this study and in Gygi's data set.

RESULTS

Profiling the Phosphoproteome in the Mouse Testis—In this study, proteome-wide profiling of phosphorylation was carried out in adult mouse testes with IMAC and TiO₂ enrichment of phosphopeptides followed by mass spectrometry identification. 12,670 and 11,309 phosphorylation sites were separately profiled from the phosphopeptides enriched by IMAC (Fig. 1A) and TiO₂ (Fig. 1B), and 6150 phosphorylation sites were enriched by both methods. In total, 17,829 phosphorylation sites in 3955 phosphoproteins were identified. The percentages of phosphoserine (pS), phosphothreonine (pT), and phosphotyrosine (pY) were ~82%, ~16%, and ~2%, respectively, which indicates that distribution patterns of the residues of the phosphorylation sites enriched by the IMAC and TiO₂ methods are similar (Fig. 1A, 1B). Because a number of phosphorylation sites were enriched by both methods, this overlap was analyzed. In total, it was found that 48.31% of the phosphorylation sites enriched by IMAC were also covered by

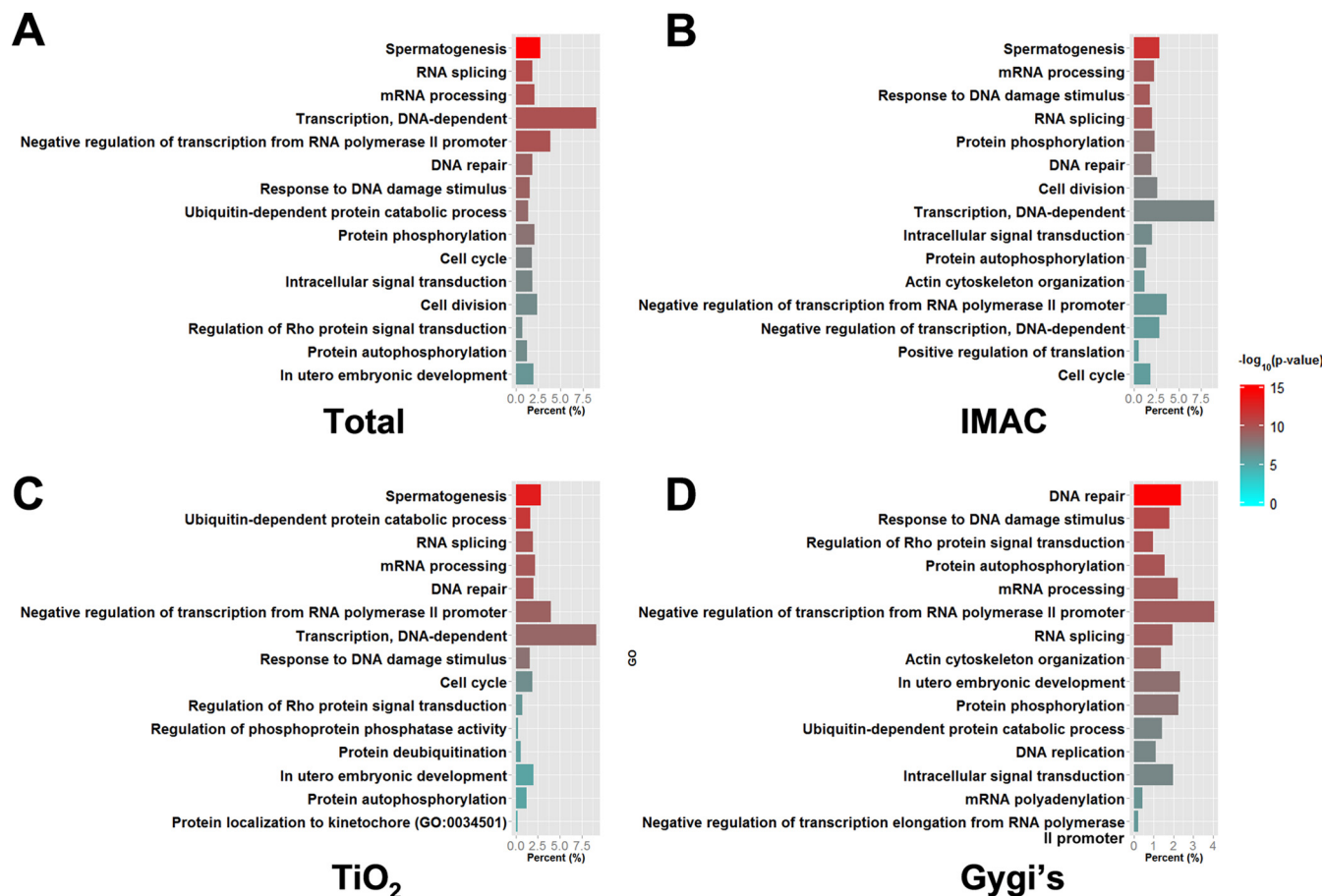


FIG. 2. Statistical analysis of the functional annotations for the phosphorylation sites identified in this study. The top 15 enriched biological processes for the total mouse testis phosphoproteome identified in this study A, or phosphorylated proteins identified by IMAC B, or TiO₂ C, or phosphorylated testis proteins identified from the Gygi's data set D. E-ratio: the proportion in the specific data set divided by that in the mouse proteome.

TiO₂ (Fig. 1C) and such a pattern of overlap is consistent with a previous study (42). The detailed results are presented in Fig. 1C, which shows the patterns of overlap in the two methods for pS and pT are similar. The overlaps among the five replicates including two replicates for IMAC and three replicates for TiO₂ were presented in supplemental Fig. S1, which showed that the overlapping ratios are limited. The details on the identified proteins, peptides, and phosphorylated sites are presented in supplemental Table S1.

Previously, Huttlin *et al.* reported a comprehensive survey of tissue-specific phosphorylation sites in nine tissues including the mouse testis (16). We retrieved the phosphopeptides identified in Huttlin *et al.* and remapped them with the mouse proteome used in this study (UniProt 2013_11). In total, 11,713 phosphorylation sites in 3087 proteins were obtained (designated as Gygi's). The overlap between Gygi's data set and our study was analyzed, and the result is presented in Fig. 1D. It was observed that only 26.58% of the phosphorylation sites in the Gygi's data set were also identified in our study (Fig. 1D). The low overlap rate might be generated from the differences between the materials used in these two studies.

First, Huttlin *et al.* used Swiss-Webster mice (16), whereas C57BL/6 mice were used in our study. Also, the phosphoproteome in Huttlin *et al.* was profiled from the testis of 3-week-old mice that did not contain elongated spermatids or spermatozoa (16), whereas the adult mouse testis were used in our study. Thus, the phosphorylation sites identified in our study more accurately represent the phosphorylation regulation events in full spermatogenesis.

Functional Annotations of the Mouse Testicular Phosphoproteome—With the comprehensive data set of testicular phosphoproteome, functional annotations of the identified phosphorylation substrates were statistically analyzed. Various data sets, including the phosphoproteomes identified in this study, that is, (Total), enriched by IMAC and TiO₂, as well as Gygi's data set were employed for statistical analysis. The enriched GO terms in these proteins were statistically analyzed with a hypergeometric pattern of distribution and the top 15 over-represented biological processes are showed in Fig. 2. It is interesting that the annotation of spermatogenesis (GO:0007283) was the most over-represented in all of the three data sets used in our study (Fig. 2A–2C). In the Gygi's

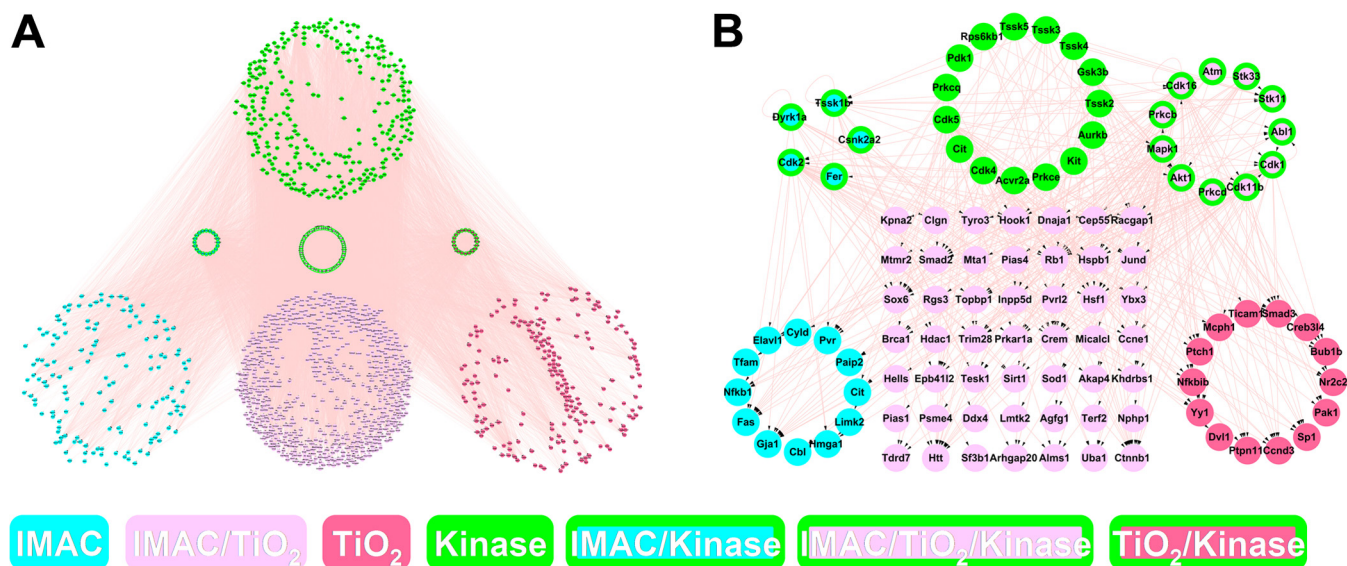


FIG. 3. Network analysis of phosphorylation regulation in the mouse testis phosphoproteome. *A*, The network constructed from the total mouse testis phosphoproteome identified in this study. *B*, The network constructed from the phosphorylated spermatogenesis-related proteins. Different colored proteins were from different data sets. “IMAC,” “TiO₂,” and “Kinase” in the colored box represent that the protein is a phosphoprotein identified by IMAC, TiO₂, and a kinase, respectively, whereas “/” means both.

data set, spermatogenesis (GO:0007283) was only a weakly over-represented annotation, with an enrichment ratio of 1.45 and a p value of 0.00226 (Data not shown), which indicates that there was only limited spermatogenesis in the testis used in Huttlin *et al.* (16). Furthermore, the cell cycle (GO:0007049) appeared in the top 15 over-represented GO terms for the phosphoproteome enriched by IMAC and TiO₂ (Fig. 2B, 2C), but not Gygi’s data set, which further demonstrates that there was no full spermatogenesis in the immature testes used by Huttlin *et al.* (16).

Apart from spermatogenesis, the phosphoproteome enriched by IMAC and TiO₂ shared a number of other annotations. For example, transcription-related processes were heavily over-represented, including RNA splicing (GO:0008380), mRNA processing (GO:0006397), negative regulation of transcription from RNA polymerase II promoter (GO:0000122), and transcription, DNA-dependent (GO:0006351) (Fig. 2B, 1C), which shows that transcription was active. The phosphoproteome from Huttlin *et al.* also had over-represented transcription-related processes, including RNA splicing (GO:0008380), mRNA processing (GO:0006397), and negative regulation of transcription from RNA polymerase II promoter (GO:0000122). The IMAC and TiO₂ data also displayed enriched DNA damage response-related processes, including DNA repair (GO:0006281) and response to DNA damage stimulus (GO:0006974), all of which were dramatically enriched in the Gygi’s data set (Fig. 2B, 1C). These results show that the DNA integrity is rigorously controlled by phosphorylation, in both spermatogenesis and testicular development. Furthermore, Protein autophosphorylation (GO:0046777) was consistently over-represented in Gygi’s data set and the phosphoproteome enriched by IMAC and TiO₂,

whereas Gygi’s data set exhibited enriched Protein phosphorylation (GO:0006468). There results show that phosphoregulation is abundant in the testis. The detailed top 15 annotations for enriched biological processes, molecular functions, and cellular components for the four data sets are presented in supplemental Table S2.

Reconstruction of the Testicular KSPN and Analysis of the Spermatogenesis-related Sub-KSPN—From the functional annotations, it is evident that the phosphoproteome profiled in this study is closely related to spermatogenesis. We further analyzed phosphoregulation by the reconstruction of the KSPNs in the testis. Using the self-developed software package iGPS (26) in the default threshold mode (Low threshold, Experimental/String PPI filter), the ssKSRs were predicted based on the total phosphoproteome identified in this study and employed to construct the KSPN (Fig. 3A, supplemental Fig. S2). In total, 3351 phosphorylation sites in 1066 substrates were predicted with at least one kinase. There were 402 kinases predicted with at least one substrate, whereas 107 kinases were identified as phosphorylated. In total, there were 17,065 KSR edges among 1393 protein nodes in the KSPN, which shows the network is as dense as ~24.5 links per node (Fig. 3A, supplemental Fig. S2).

To further explore phosphoregulation in spermatogenesis, the sub-KSPN among the spermatogenesis-related proteins was constructed. The spermatogenesis-related proteins were retrieved from the QuickGO database (40) with annotations for spermatogenesis (GO:0007283) and the proteins in the SpermatogenesisOnline database (43) were also collected. All of these proteins were integrated with the KSPN to retrieve the sub-KSPN (Fig. 3B, supplemental Fig. S3). There were 106 proteins and 371 predicted KSRs in the sub-KSPN, which

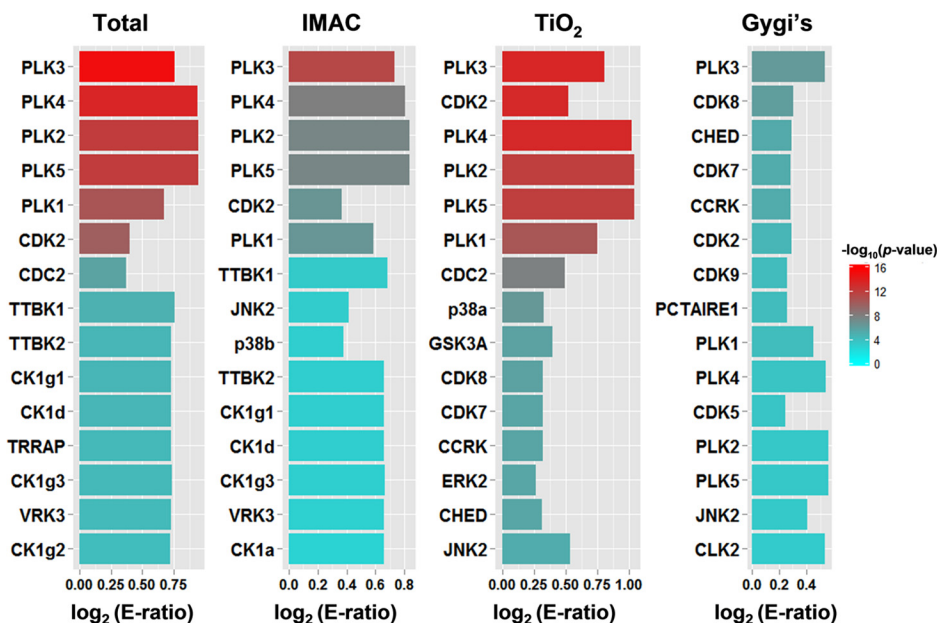


FIG. 4. **The kinase activity analyses for the phosphoproteomes.** The top15 significantly high-activity kinases for the total mouse testis phosphoproteome identified in this study *A*, or phosphorylated proteins identified by IMAC *B*, or TiO₂ *C*, or phosphorylated testis proteins identified from the Gygi's data set *D*, are presented (p value < 0.05). E-ratio: the proportion in the specific data set divided by that in the mouse phosphoproteome atlas.

indicates that the sub-KSPN is denser than the KSPN. Previously, it was reported that the MPAKs play an important role in spermatogenesis (6), with MAPK1 predicted to phosphorylate 47 (~44%) proteins in the sub-KSPN (supplemental Fig. S4).

Because the KSPN is the first kinase-substrate phosphorylation network specifically constructed for spermatogenesis in the testis, the predicted ssKSRs in the network would be expected to provide helpful information for further studies. In order to provide user-friendly accession of the data, the database of pTestis was constructed and is available at <http://ptestis.biocuckoo.org>. All of the identified phosphorylation sites were integrated along with UniProt annotations (38) into the database, with snapshots of the database presented in supplemental Fig. S5. Users may quickly perform various searches such as a keyword-based query (supplemental Fig. S5A, S5B) and sequence-based blast (supplemental Fig. S5C). If the kinases were predicted by iGPS for the phosphorylation site, the detailed results may be seen by clicking "View/Close" (supplemental Fig. S5D).

Prediction of Kinases with Differential Activities in Order to Reveal Potentially Important Regulators in Spermatogenesis— Because the testicular phosphoproteome profiled in this study is closely related with spermatogenesis and kinases are the enzymes responsible for the phosphorylation process, the main kinases for the phosphoproteome might be the key regulators of testis and spermatogenesis. As previously described (26), the kinase activity in the phosphoproteome was computed as the number of predicted ssKSRs in the KSPN. Furthermore, to distinguish the testis-specific high-activity

kinases, the average kinase activities calculated from mouse atlas phosphoproteome in the Huttlin *et al.* (16) were employed as the background. The top15 kinases with significantly high activities for four data set including Total, IMAC, TiO₂, and Gygi's are presented in Fig. 4, with the details provided in supplemental Table S3.

It is clear from the results that although the overlap of the phosphoproteome in these data sets is not high, the top15 high-activity kinases were nevertheless consistent. Generally, high-activity kinases with more ssKSRs are considered as more important, whereas kinases with significantly high activity in the KSPN through a statistical comparison with kinase activities in the mouse atlas are considered to be the key kinases in the testis. For example, the MAPKs were identified as important kinases during spermatogenesis (6), and here it was shown that the MAPKs, including JNK2, ERK2, and p38s, had a consistently high level of activity in the four data sets (supplemental Table 3). Previously, CDK2 was identified as important for homologous chromosomes to undergo accurate pairing and recombination during meiosis in the testis (44). Here it is shown that CDK2 was consistently found among the top15 high-activity kinases in all four data sets (Fig. 4, supplemental Table S3). Recently, Shi *et al.* proposed that CDC2 makes a critical contribution to both sperm activity and testicular function (19), whereas the results from the Total and TiO₂ data sets showed that CDC2 was among the top15 high-activity kinases (Fig. 4, supplemental Table S3). Furthermore, the kinase activity profiles for the five replicates were also predicted separately and presented in supplemental Fig. S6, which showed that although the overlapping ratios for

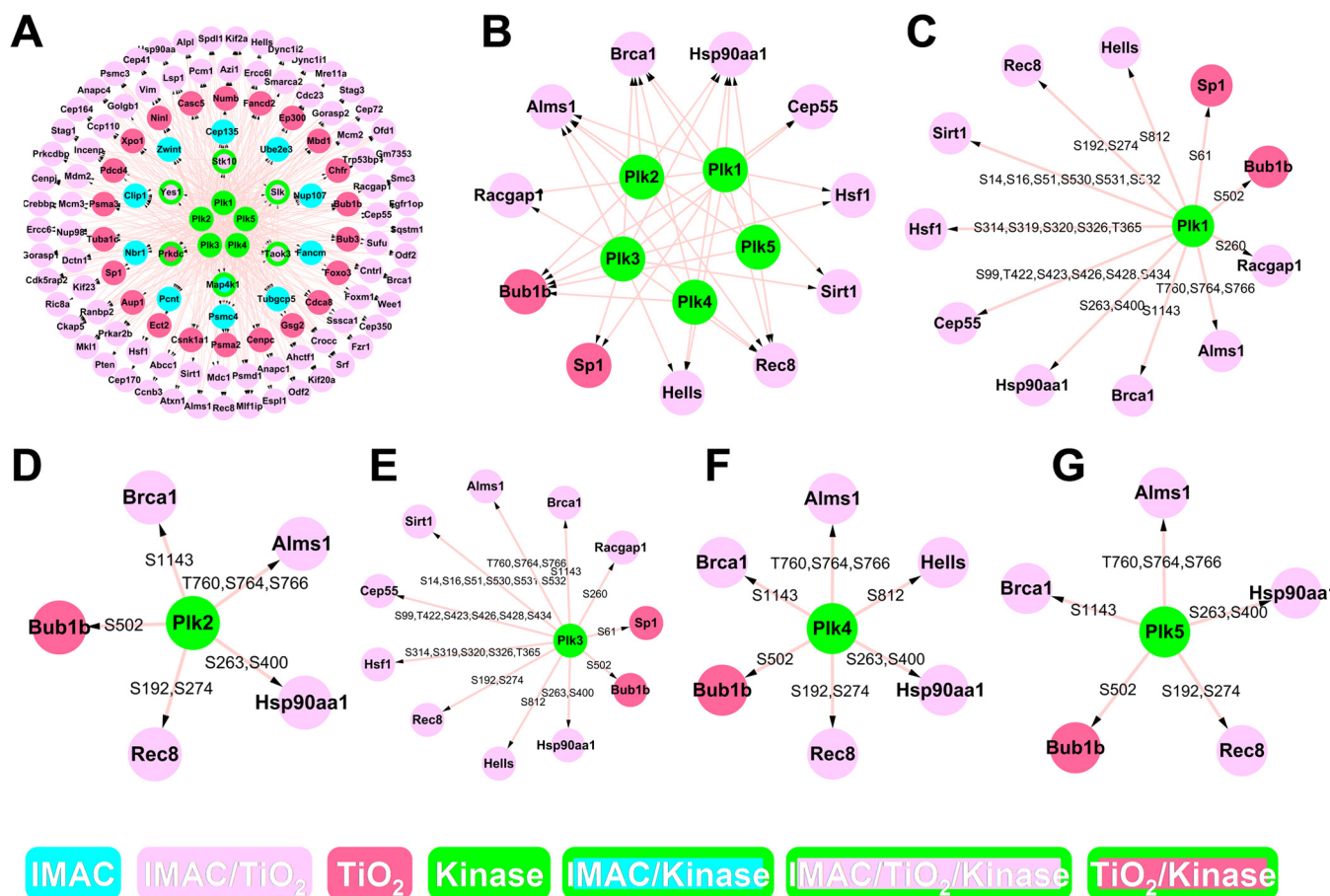


FIG. 5. The phosphorylation network for the PLKs. *A*, The phosphorylation network among the PLKs and the substrates of the PLKs. *B*, The phosphorylation network among the PLKs and the PLKs phosphorylated spermatogenesis-related proteins. The phosphorylation network annotated with identified sites for PLK1 *C*, PLK2 *D*, PLK3 *E*, PLK4 *F*, and PLK5 *G*. Different colored proteins were from different data sets. “IMAC,” “TiO₂,” and “Kinase” in the colored box represent that the protein is a phosphoprotein identified by IMAC, TiO₂, and a kinase, respectively, whereas “/” means both.

sites identifications is not high, the kinase activity profiles were consistent. The consistency between the findings here and previous studies indicate that the network-based KAA method is able to identify key regulators in biological samples.

The Significantly Higher Activities of the PLKs and the Implications for Spermatogenesis—Perhaps the most striking result of the KAA predictions is that the PLKs were consistently among the top15 high-activity kinases in all four data sets (Fig. 4, supplemental Table S3). Furthermore, the results from the data sets in this study were more significant than the Gygi’s data set. Because the functional annotations analyses showed that the phosphoproteome in this study was more closely related with spermatogenesis than Huttlin *et al.* (16), it is suggested that the PLKs might be key regulators in spermatogenesis. Because the high activity level implies the importance of the PLKs, it is important to analyze the PLK sub-KSPN. There were 122 proteins with 499 predicted KSRs in the PLK sub-KSPN (Fig. 5A, supplemental Fig. S7), and it is interesting that 83 of the 117 (~71%) phosphorylated substrates were enriched in both IMAC and TiO₂. Although PLKs

were not annotated as spermatogenesis-related in the gene ontology database (40) or SpermatogenesisOnline database (43), a number of spermatogenesis-related proteins were predicted to be regulated by PLKs in our study. The PLK-regulated spermatogenesis-related sub-KSPN is presented in Fig. 5B, and there were abundant overlapped substrates among the different PLKs, including Alms1, Bub1b, Brca1, Hsp99aa1, and Rec8. The PLK subtype-specific regulated spermatogenesis-related sub-KSPNs are presented in Fig. 5C–5G, which show that PLK1 regulates more substrates than the other subtypes.

To further understand the functional implications of the PLKs in spermatogenesis, the phenotype and disease associations from the MGI database (45) for the predicted PLK substrates were analyzed by ToppGene (46). The top8 associations (p value $< 10^{-6}$) of the statistical results were shown in Table II. It was found that the most significantly associated phenotypes for the PLK substrates were cell morphology related, including abnormal cell nucleus morphology (MP: 0003111) and abnormal cell morphology (MP:0000358). Also,

TABLE II
The phenotype and disease associations for the substrates of PLKs in MGI database

Phenotype ID	Description	p value
MP:0003111	Abnormal cell nucleus morphology	2.26E-10
MP:0003077	Abnormal cell cycle	5.71E-08
MP:0004046	Abnormal mitosis	8.76E-08
MP:0000358	Abnormal cell morphology	3.10E-07
MP:0002022	Increased lymphoma incidence	3.97E-07
MP:0002020	Increased tumor incidence	4.03E-07
MP:0010274	Increased organ/body region tumor incidence	5.83E-07
MP:0002019	Abnormal tumor incidence	9.06E-07

cell proliferation related annotations, including abnormal cell cycle (MP:0003077) and abnormal mitosis (MP:0004046) were significantly associated with the PLK substrates. Disease associations, including increased lymphoma incidence (MP:0002022), increased tumor incidence (MP:0002020), increased organ/body region tumor incidence (MP:0010274), and abnormal tumor incidence (MP:0002019) were closely related with the PLK substrates. Taken together, our results suggested that the PLK substrates were highly implicated in cell cycle and PLKs might play a potential role during cell proliferation in the mouse testis.

Validation of the Activation and Importance of the PLKs— The computational analyses indicated potentially higher activities of PLKs in adult testes, whereas the predictions should be experimentally validated. Previous studies showed that the phosphorylated threonine 210 (pT210) is a major phosphorylation site in PLK1 and its phosphorylation level is correlated with the activation of PLK1 (29, 30). Thus, both the expression and pT210 phosphorylation of PLK1 were examined by Western blot analysis to verify the different activities of PLK1 in testes against other tissues. Because the PLK1 activity was predicted to be higher in mature mouse testes in this study than 3-week mouse testes in Huttlin *et al.* (16), testes of different developmental stages including 1-week, 2-week, 3-week, 4-week, and adult (8-week) mice were analyzed. The mixtures of eight tissues including brain, brown fat, heart, liver, lung, kidney, pancreas, and spleen from 3-week and 8-week mice were employed as the control, which is consistent with the computational analyses. The result showed that the activity of PLK1 in testis increased as testis matures with age, and was higher than the control of tissue mixtures (Fig. 6A). Interestingly, the expression of PLK1 in testis also increased with age (Fig. 6A), which indicated that the high PLK1 activity might be because of the high expression level of PLK1. Taken together, there were indeed high activity of PLK1 in mature testis compared with immature testis and averaged other tissues, which validated the computational prediction.

Because the activity analyses of PLK by detecting phosphorylation showed high activity in mature testis, we performed further *in vitro* inhibition assay to study the role of the

PLKs in spermatogenesis. The GC2 cell line, which is a spermatocyte cell line, was employed in this study for experimental purposes. The small-molecule inhibitor BI2536 was employed to characterize the effects of PLK inhibition. BI2536 has specificity for the PLKs, including PLK1, PLK2, and PLK3 but cannot distinguish the subtypes. The expression levels of PLK1, PLK2, and PLK3 mRNAs were analyzed by RT-PCR and the results are presented in supplemental Fig. S8, which show that they are all expressed. The effects of PLK inhibition were surveyed with the help of a Fluorescence Activated Cell Sorting (FACS) system. It was observed that, at 2 h (2h), 4 h (4h), and 6 h (6h) after treatment of GC2 cells with 100 nM BI2536, cell cycle G2/M arrest was induced (Fig. 6B–6D). In comparison with the control which received only DMSO, the percentage of cells in the G2/M phase with BI 2536 increased from 18.3% (4h) and 13.6% (6h) to 28.5% (4h, $p < 0.01$) and 31.5% (6h, $p < 0.01$), respectively (Fig. 6C, 6D). In the control, there was no significant change in the percentage of cells in the G1 phase or S phase at 2h or 4h after treatment, except that the G1 stage cells decreased 6h after treatment. These results show that BI2536 induced arrest in the G2/M phase and inhibited cell proliferation.

To further study whether the observed G2/M arrest is caused by the inhibition of the kinase activity of PLK1–3, we employed the phosphatase inhibitor okadaic acid (OA), which was reported to reverses the phosphorylation changes that occur after inhibition of PLKs. FACS analysis showed that, in comparison with those without OA, at 4h and 6h after 1 μ M OA treatment of GC2 cells together with BI2536, the percentage of cells in G2/M decreased from 28.5% (4h) and 31.5% (6h) to 21.6% (4h, $p < 0.05$) and 23.3% (6h, $p < 0.01$), respectively (Fig. 6C, 6D). The percentage of cells in the S phase was not significantly different between these two groups. The G1 phase increased from 24.2% to 35.8% ($p < 0.01$) 6h after treatment when 1 μ M OA was used together with BI2536 (Fig. 6C, 6D). These findings show that OA is able to reverse the G2/M arrest caused by BI2536. As OA is a type of phosphatase inhibitor and BI2536 acts as a kinase inhibitor against PLK1–3, the G2/M arrest is regulated by these two inhibitors in opposite ways. Thus, the kinase activity of PLK1–3 is crucial for cell cycle regulation in this spermatocyte cell line.

DISCUSSION

Spermatogenesis is a complex process critical for mammalian reproduction and we hypothesized that a detailed study of the testis might provide in-depth understanding of the underlying molecular mechanisms. As the most well characterized PTM, phosphorylation has been reported to play an important role in almost all cellular processes (47). Recently, state-of-the-art MS based proteome-scale identification of phosphorylation events, especially computationally based phosphoproteome studies, have become sufficiently advanced to provide comprehensive analyses of phosphoregulation (8, 20, 22, 26). To further understand the molecular mechanisms of

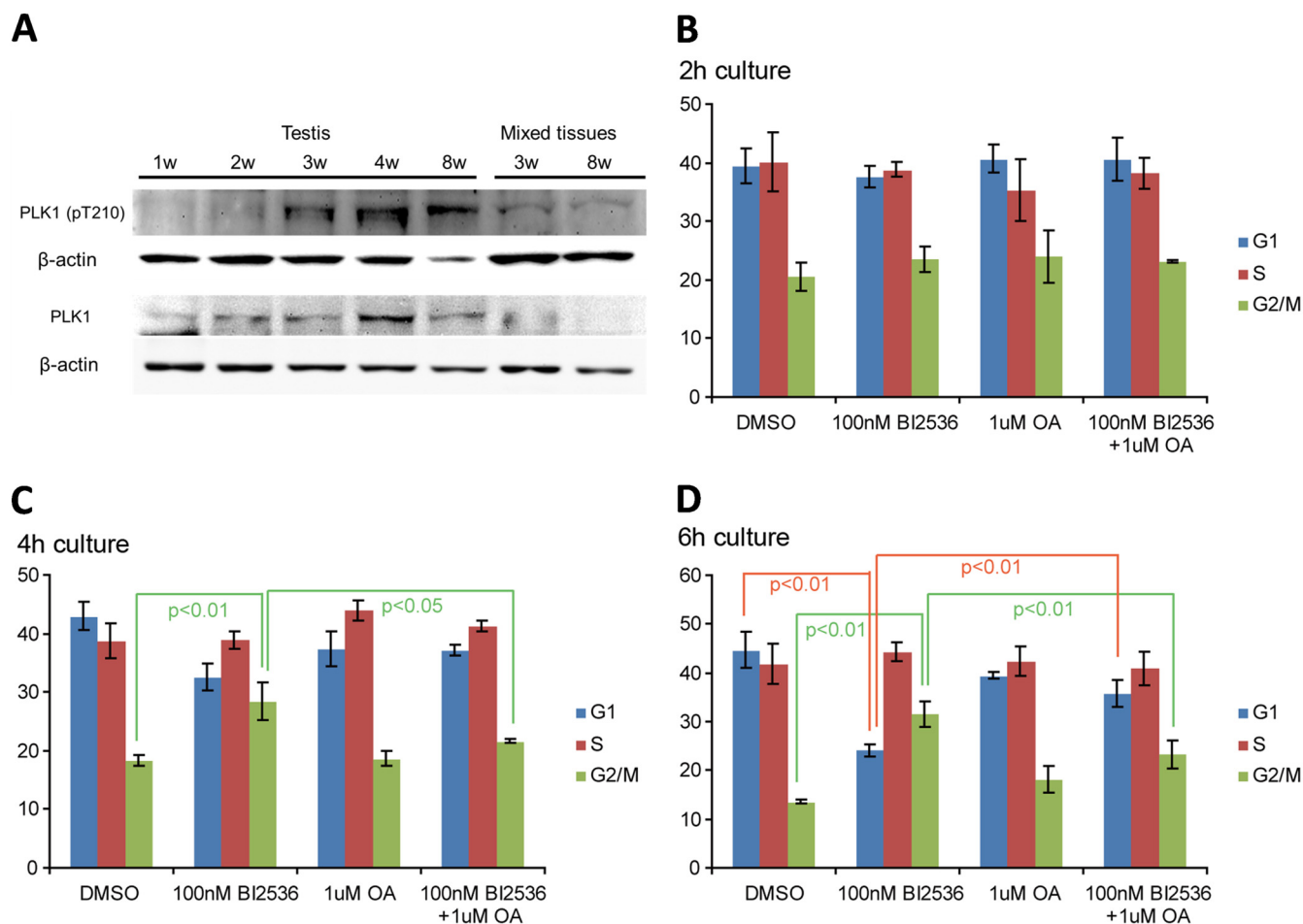


FIG. 6. **The phosphorylation level of PLK1 and inhibition assay of the PLKs in GC2 cells.** A, The expression and pT210 levels of PLK1 in testes and mixed tissues of different developmental stages were analyzed by Western blot, with β actin as a loading control. Mixed tissues is the pooling of equal amount of brain, brown fat, heart, liver, lung, kidney, pancreas, and spleen from 3-week or 8-week mice. The distribution patterns of GC2 cells in different phases of the cell cycle were compared after treatment with BI2536 and/or OA for 2 h B, 4 h C, and 6 h D.

spermatogenesis, it would be of great value to have data on the phosphoproteome in the testis. In this study, we systematically profiled the testicular phosphoproteome. The 17,829 phosphorylation sites in the 3955 proteins identified are currently the largest phosphorylation data set in the testis. The samples were prepared from adult mouse testes and the functional annotations show that the identified substrates are closely related to spermatogenesis. These results further demonstrate that spermatogenesis is extensively regulated by phosphorylation. Compared with the phosphoproteome profiled from the 3-week-old mouse testis in Huttlin *et al.* (16), these results provide a more accurate picture of phosphorylation regulation in spermatogenesis.

Previous literatures have shown that alternative splicing is extensive in the testis (48, 49). Alternative splicing generates different mature transcripts and protein variants, sometimes with adverse functions (50). A microarray study of human exons also showed that the testis has the second highest number of tissue-specific exons, a number that is only moderately smaller than the brain (51), and the second highest

number of cassette exons (49, 52). Furthermore, a cDNA microarray study indicated that alternative splicing is important for both testis development and spermatogenesis (53). In our study, functional annotation of the identified phosphoproteome showed that RNA splicing is high enriched, which suggests that phosphorylation may be critical for the regulation of alternative splicing in spermatogenesis. Furthermore, apart from transcription, in the testis there is a well-known phenomenon of “translational delay” in which mRNA expression alone does not ensure the existence of the corresponding protein (54). The deregulation of translation can lead to a failure of spermatogenesis. For example, in transgenic mice, because the protamine mRNA derived was translated prematurely because of the lack of the 3' UTR region essential for translational regulation, the animals were completely infertile (55). The enrichment of various annotations for transcription and translation indicated that translational regulation in spermatogenesis may also be regulated by phosphorylation.

In this study, PLKs were predicted as high-activity kinases, indicating that the PLKs are key regulators in the testis and

thus implicated to have a role in spermatogenesis. Previously, PLKs were characterized as critical for the cell cycle (7, 8) and required in spermatogenesis (9–12). It was suggested in this study that the PLKs appear to play a pivotal role in the testis through regulation of the phosphoproteome, a finding that was consistently observed in all of the data sets analyzed, including phosphoproteome enriched by IMAC and TiO₂ in this study as well as Gygi's data set. To validate the findings, the high-activities of PLKs should be examined. Previously Yu *et al.* developed the KAYAK strategy to systematically profile the activation of kinases through detecting the phosphorylation of kinase-specific peptide substrates (56). This approach was further extended by Kubota *et al.* to simultaneously monitor kinase activities in a state-of-art manner and perform activity-based kinase identification (57). However, for one or several kinases, detection of the activity-associated phosphorylation sites in kinases could serve as an alternative way to sense the activation of kinases (28). Previously, Lee *et al.* found that mimicking phosphorylation of T210 by mutation to glutamic acid (T210D) could elevate the activity of PLK1 (31). Further study on *Xenopus* Plx1 (homologous to PLK1) by Kelm *et al.* discovered two potential autophosphorylation sites including S260 and S326, and two other phosphorylation sites including T201 (homologous to T210 in PLK1) and S340, whereas phosphorylation of T201 was identified as the major event for activation of Plx1 (30). These observations were consistent with following study by Jang *et al.* (29). Recently, it was observed that the phosphorylation of T210 by aurora A is required for PLK1 to promote mitotic entry, whereas T210D mutation partially overcomes the absence of aurora A (32). Taken together, pT210 was critical for the activation of PLK1, whereas Western blot results showed a higher activity of PLK1 in mature testes compare with in immature testes and tissue mixtures.

Furthermore, the importance of PLKs in testis and spermatogenesis was validated through inhibition assay using BI2536 in a spermatocyte GC2 cell line. Previously, PLK1 was reported to be important for the G2/M checkpoint (58), so the increase of cells in the G2/M stage may be caused by the inhibition of PLK1. The inhibition in the GC2 cells can be reversed by the phosphatase inhibitor OA. Thus, the inhibition of cell cycle progression is caused by the inhibition of the kinase activity of the PLKs. In fact, Jordan *et al.* have discovered the great importance of PLKs in synaptonemal complex disassembly in mouse spermatocytes by brief *in vitro* culture of spermatocytes (12). Recently, Cdc5, an ortholog of the PLKs, was found to be a central regulator of meiosis I in yeast (59). Taking these various points into consideration, it is proposed that the PLKs are critical for spermatogenesis. Further studies of PLK mediated phosphoregulation should prove to be of great value for understanding of the molecular mechanisms of spermatogenesis.

Taking the findings together, this study provides a comprehensive phosphoproteome data set in the testis and a land-

scape of phosphoregulation of spermatogenesis. Inspired by a computational approach, a number of kinases were proposed as key regulators for spermatogenesis, a handful of which were consistent with previous findings, and the importance of the PLKs was corroborated by experimental results. We believe that the phosphoregulation and kinase activity results in this study will prove to be of great help for further studies of both the testis and spermatogenesis.

Acknowledgments—We thank the PRIDE team for the support of data deposition to the ProteomeXchange Consortium, and Pacific Edit for the review of the manuscript prior to submission.

* This work was supported by grants from the Chinese Natural Science Funds (81222006), the 973 program (2013CB933900, 2013CB947902, 2012CB910101, and 2011CB944304), the Chinese Natural Science Funds (31271245, 31171263, 31471403, and 81272578), International Science & Technology Cooperation Program of China (2014DFB30020), China Postdoctoral Science Foundation (2014M550392) and the Natural Science Foundation of the Jiangsu Higher Education Institutions of China (Grant No. 13KJA310002).

¶ To whom correspondence should be addressed: Dr. Xuejiang Guo, Tel.: +86-25-86862038, Fax: +86-25-86862908, E-mail: guo_xuejiang@njmu.edu.cn; Dr. Yu Xue, Tel.: +86-27-87793903, Fax: +86-27-87793172, E-mail: xueyu@mail.hust.edu.cn.

§ This article contains supplemental Figs. S1 to S8 and Tables S1 to S3.

|| These authors contributed equally to the work.

REFERENCES

- Braun, R. E. (1998) Every sperm is sacred—or is it? *Nat. Genet.* **18**, 202–204
- Liu, M., Hu, Z., Qi, L., Wang, J., Zhou, T., Guo, Y., Zeng, Y., Zheng, B., Wu, Y., Zhang, P., Chen, X., Tu, W., Zhang, T., Zhou, Q., Jiang, M., Guo, X., Zhou, Z., and Sha, J. (2013) Scanning of novel cancer/testis proteins by human testis proteomic analysis. *Proteomics* **13**, 1200–1210
- Guo, X., Zhang, P., Huo, R., Zhou, Z., and Sha, J. (2008) Analysis of the human testis proteome by mass spectrometry and bioinformatics. *Proteomics Clin. Appl.* **2**, 1651–1657
- Guo, X., Zhao, C., Wang, F., Zhu, Y., Cui, Y., Zhou, Z., Huo, R., and Sha, J. (2010) Investigation of human testis protein heterogeneity using 2-dimensional electrophoresis. *J. Androl.* **31**, 419–429
- Fisher, D., Krasinska, L., Coudreuse, D., and Novak, B. (2012) Phosphorylation network dynamics in the control of cell cycle transitions. *J. Cell Sci.* **125**, 4703–4711
- Li, M. W., Mruk, D. D., and Cheng, C. Y. (2009) Mitogen-activated protein kinases in male reproductive function. *Trends Mol. Med.* **15**, 159–168
- Nigg, E. A. (1998) Polo-like kinases: positive regulators of cell division from start to finish. *Curr. Opin. Cell Biol.* **10**, 776–783
- Liu, Z., Ren, J., Cao, J., He, J., Yao, X., Jin, C., and Xue, Y. (2013) Systematic analysis of the Plk-mediated phosphoregulation in eukaryotes. *Brief Bioinform.* **14**, 344–360
- Matsubara, N., Yanagisawa, M., Nishimune, Y., Obinata, M., and Matsui, Y. (1995) Murine polo like kinase 1 gene is expressed in meiotic testicular germ cells and oocytes. *Mol. Reprod. Dev.* **41**, 407–415
- Carmena, M., Riparbelli, M. G., Ministrini, G., Tavares, A. M., Adams, R., Callaini, G., and Glover, D. M. (1998) Drosophila polo kinase is required for cytokinesis. *J. Cell Biol.* **143**, 659–671
- Bettencourt-Dias, M., Rodrigues-Martins, A., Carpenter, L., Riparbelli, M., Lehmann, L., Gatt, M. K., Carmo, N., Balloux, F., Callaini, G., and Glover, D. M. (2005) SAK/PLK4 is required for centriole duplication and flagella development. *Curr. Biol.* **15**, 2199–2207
- Jordan, P. W., Karppinen, J., and Handel, M. A. (2012) Polo-like kinase is required for synaptonemal complex disassembly and phosphorylation in mouse spermatocytes. *J. Cell Sci.* **125**, 5061–5072
- Doerr, A. (2012) Making PTMs a priority. *Nat. Methods* **9**, 862–863
- Baker, M. A., Smith, N. D., Hetherington, L., Pelzing, M., Condina, M. R.,

- and Aitken, R. J. (2011) Use of titanium dioxide to find phosphopeptide and total protein changes during epididymal sperm maturation. *J. Proteome Res.* **10**, 1004–1017
15. Baker, M. A., Smith, N. D., Hetherington, L., Taubman, K., Graham, M. E., Robinson, P. J., and Aitken, R. J. (2010) Label-free quantitation of phosphopeptide changes during rat sperm capacitation. *J. Proteome Res.* **9**, 718–729
 16. Huttlin, E. L., Jedrychowski, M. P., Elias, J. E., Goswami, T., Rad, R., Beausoleil, S. A., Villen, J., Haas, W., Sowa, M. E., and Gygi, S. P. (2010) A tissue-specific atlas of mouse protein phosphorylation and expression. *Cell* **143**, 1174–1189
 17. Parte, P. P., Rao, P., Redij, S., Lobo, V., D'Souza, S. J., Gajbhiye, R., and Kulkarni, V. (2012) Sperm phosphoproteome profiling by ultra performance liquid chromatography followed by data independent analysis (LC-MS(E)) reveals altered proteomic signatures in asthenozoospermia. *J. Proteomics* **75**, 5861–5871
 18. Porambo, J. R., Salicioni, A. M., Visconti, P. E., and Platt, M. D. (2012) Sperm phosphoproteomics: historical perspectives and current methodologies. *Expert Rev. Proteomics* **9**, 533–548
 19. Shi, Z., Hou, J., Guo, X., Zhang, H., Yang, F., and Dai, J. (2013) Testicular phosphoproteome in perfluorododecanoic acid-exposed rats. *Toxicol. Lett.* **221**, 91–101
 20. Liu, Z., Wang, Y., and Xue, Y. (2013) Phosphoproteomics-based network medicine. *FEBS J.* **280**, 5696–5704.
 21. Xue, Y., Liu, Z., Cao, J., and Ren, J. (2011) Computational Prediction of Post-Translational Modification Sites in Proteins. In: Yang, N.-S., ed. *Systems and Computational Biology - Molecular and Cellular Experimental Systems*, InTech., Rijeka, Croatia. **6**, 106–127
 22. Ren, J., Gao, X., Liu, Z., Cao, J., Ma, Q., and Xue, Y. (2011) Computational analysis of phosphoproteomics: progresses and perspectives. *Curr. Protein Pept. Sci.* **12**, 591–601
 23. Xue, Y., Gao, X., Cao, J., Liu, Z., Jin, C., Wen, L., Yao, X., and Ren, J. (2010) A summary of computational resources for protein phosphorylation. *Curr. Protein Pept. Sci.* **11**, 485–496
 24. Linding, R., Jensen, L. J., Ostheimer, G. J., van Vugt, M. A., Jorgensen, C., Miron, I. M., Diella, F., Colwill, K., Taylor, L., Elder, K., Metalnikov, P., Nguyen, V., Pasculescu, A., Jin, J., Park, J. G., Samson, L. D., Woodgett, J. R., Russell, R. B., Bork, P., Yaffe, M. B., and Pawson, T. (2007) Systematic discovery of in vivo phosphorylation networks. *Cell* **129**, 1415–1426
 25. Linding, R., Jensen, L. J., Pasculescu, A., Olhovsky, M., Colwill, K., Bork, P., Yaffe, M. B., and Pawson, T. (2008) NetworKIN: a resource for exploring cellular phosphorylation networks. *Nucleic Acids Res.* **36**, D695–699
 26. Song, C., Ye, M., Liu, Z., Cheng, H., Jiang, X., Han, G., Songyang, Z., Tan, Y., Wang, H., Ren, J., Xue, Y., and Zou, H. (2012) Systematic analysis of protein phosphorylation networks from phosphoproteomic data. *Mol. Cell Proteomics* **11**, 1070–1083
 27. Zanivan, S., Meves, A., Behrendt, K., Schoof, E. M., Neilson, L. J., Cox, J., Tang, H. R., Kalna, G., van Ree, J. H., van Deursen, J. M., Trempus, C. S., Machesky, L. M., Linding, R., Wickstrom, S. A., Fassler, R., and Mann, M. (2013) In vivo SILAC-based proteomics reveals phosphoproteome changes during mouse skin carcinogenesis. *Cell Rep.* **3**, 552–566
 28. Casado, P., Rodriguez-Prados, J. C., Cosulich, S. C., Guichard, S., Vanhaesebroeck, B., Joel, S., and Cutillas, P. R. (2013) Kinase-substrate enrichment analysis provides insights into the heterogeneity of signaling pathway activation in leukemia cells. *Sci. Signal* **6**, rs6
 29. Jang, Y. J., Ma, S., Terada, Y., and Erikson, R. L. (2002) Phosphorylation of threonine 210 and the role of serine 137 in the regulation of mammalian polo-like kinase. *J. Biol. Chem.* **277**, 44115–44120
 30. Kelm, O., Wind, M., Lehmann, W. D., and Nigg, E. A. (2002) Cell cycle-regulated phosphorylation of the *Xenopus* polo-like kinase Plx1. *J. Biol. Chem.* **277**, 25247–25256
 31. Lee, K. S., and Erikson, R. L. (1997) Plk is a functional homolog of *Saccharomyces cerevisiae* Cdc5, and elevated Plk activity induces multiple septation structures. *Mol. Cell Biol.* **17**, 3408–3417
 32. Macurek, L., Lindqvist, A., Lim, D., Lampson, M. A., Klompmaker, R., Freire, R., Clouin, C., Taylor, S. S., Yaffe, M. B., and Medema, R. H. (2008) Polo-like kinase-1 is activated by aurora A to promote checkpoint recovery. *Nature* **455**, 119–123
 33. Villen, J., and Gygi, S. P. (2008) The SCX/IMAC enrichment approach for global phosphorylation analysis by mass spectrometry. *Nat. Protoc.* **3**, 1630–1638
 34. Wu, J., Shakey, Q., Liu, W., Schuller, A., and Follettie, M. T. (2007) Global profiling of phosphopeptides by titania affinity enrichment. *J. Proteome Res.* **6**, 4684–4689
 35. Li, Q. R., Ning, Z. B., Tang, J. S., Nie, S., and Zeng, R. (2009) Effect of peptide-to-TiO₂ beads ratio on phosphopeptide enrichment selectivity. *J. Proteome Res.* **8**, 5375–5381
 36. Rappsilber, J., Mann, M., and Ishihama, Y. (2007) Protocol for micro-purification, enrichment, pre-fractionation, and storage of peptides for proteomics using StageTips. *Nat. Protoc.* **2**, 1896–1906
 37. Cox, J., and Mann, M. (2008) MaxQuant enables high peptide identification rates, individualized p.p.b.-range mass accuracies and proteome-wide protein quantification. *Nat. Biotechnol.* **26**, 1367–1372
 38. Consortium., U. (2013) Update on activities at the Universal Protein Resource (UniProt) in 2013. *Nucleic Acids Res.* **41**, D43–47
 39. Vizcaino, J. A., Cote, R. G., Csordas, A., Dianes, J. A., Fabregat, A., Foster, J. M., Griss, J., Alpi, E., Birim, M., Contell, J., O'Kelly, G., Schoenegger, A., Ovelleiro, D., Perez-Riverol, Y., Reisinger, F., Rios, D., Wang, R., and Hermjakob, H. (2013) The PRoteomics IDentification (PRIDE) database and associated tools: status in 2013. *Nucleic Acids Res.* **41**, D1063–1069
 40. Binns, D., Dimmer, E., Huntley, R., Barrell, D., O'Donovan, C., and Apweiler, R. (2009) QuickGO: a web-based tool for Gene Ontology searching. *Bioinformatics* **25**, 3045–3046
 41. Smoot, M. E., Ono, K., Ruscheinski, J., Wang, P. L., and Ideker, T. (2011) Cytoscape 2.8: new features for data integration and network visualization. *Bioinformatics* **27**, 431–432
 42. Bodenmiller, B., Mueller, L. N., Mueller, M., Domon, B., and Aebersold, R. (2007) Reproducible isolation of distinct, overlapping segments of the phosphoproteome. *Nat. Methods* **4**, 231–237
 43. Zhang, Y., Zhong, L., Xu, B., Yang, Y., Ban, R., Zhu, J., Cooke, H. J., Hao, Q., and Shi, Q. (2013) SpermatogenesisOnline 1.0: a resource for spermatogenesis based on manual literature curation and genome-wide data mining. *Nucleic Acids Res.* **41**, D1055–1062
 44. Viera, A., Rufas, J. S., Martinez, I., Barbero, J. L., Ortega, S., and Suja, J. A. (2009) CDK2 is required for proper homologous pairing, recombination and sex-body formation during male mouse meiosis. *J. Cell Sci.* **122**, 2149–2159
 45. Blake, J. A., Bult, C. J., Eppig, J. T., Kadin, J. A., Richardson, J. E., and Mouse Genome Database, G. (2014) The Mouse Genome Database: integration of and access to knowledge about the laboratory mouse. *Nucleic Acids Res.* **42**, D810–817
 46. Chen, J., Bardes, E. E., Aronow, B. J., and Jegga, A. G. (2009) ToppGene Suite for gene list enrichment analysis and candidate gene prioritization. *Nucleic Acids Res.* **37**, W305–311
 47. Walsh, C. (2005) *Posttranslational Modification of Proteins: Expanding Nature's Inventory*, Roberts and Co. Publishers, Greenwood Village, Colorado.
 48. Venables, J. P. (2002) Alternative splicing in the testes. *Curr. Opin. Genet. Dev.* **12**, 615–619
 49. Yeo, G., Holste, D., Kreiman, G., and Burge, C. B. (2004) Variation in alternative splicing across human tissues. *Genome Biol.* **5**, R74
 50. Zhu, H., Zhu, J. X., Lo, P. S., Li, J., Leung, K. M., Rowlands, D. K., Tsang, L. L., Yu, M. K., Jiang, J. L., Lam, S. Y., Chung, Y. W., Zhou, Z., Sha, J., and Chang Chan, H. (2003) Rescue of defective pancreatic secretion in cystic-fibrosis cells by suppression of a novel isoform of phospholipase C. *Lancet* **362**, 2059–2065
 51. Clark, T. A., Schweitzer, A. C., Chen, T. X., Staples, M. K., Lu, G., Wang, H., Williams, A., and Blume, J. E. (2007) Discovery of tissue-specific exons using comprehensive human exon microarrays. *Genome Biol.* **8**, R64
 52. Elliott, D. J., and Grellscheid, S. N. (2006) Alternative RNA splicing regulation in the testis. *Reproduction* **132**, 811–819
 53. Huang, X., Li, J., Lu, L., Xu, M., Xiao, J., Yin, L., Zhu, H., Zhou, Z., and Sha, J. (2005) Novel development-related alternative splices in human testis identified by cDNA microarrays. *J. Androl.* **26**, 189–196
 54. Kleene, K. C. (1996) Patterns of translational regulation in the mammalian testis. *Mol. Reprod. Dev.* **43**, 268–281
 55. Lee, K., Haugen, H. S., Clegg, C. H., and Braun, R. E. (1995) Premature translation of protamine 1 mRNA causes precocious nuclear condens-

- tion and arrests spermatid differentiation in mice. *Proc. Natl. Acad. Sci. U.S.A.* **92**, 12451–12455
56. Yu, Y., Anjum, R., Kubota, K., Rush, J., Villen, J., and Gygi, S. P. (2009) A site-specific, multiplexed kinase activity assay using stable-isotope dilution and high-resolution mass spectrometry. *Proc. Natl. Acad. Sci. U.S.A.* **106**, 11606–11611
57. Kubota, K., Anjum, R., Yu, Y., Kunz, R. C., Andersen, J. N., Kraus, M., Keilhack, H., Nagashima, K., Krauss, S., Paweletz, C., Hendrickson, R. C., Feldman, A. S., Wu, C. L., Rush, J., Villen, J., and Gygi, S. P. (2009) Sensitive multiplexed analysis of kinase activities and activity-based kinase identification. *Nat. Biotechnol.* **27**, 933–940
58. de Carcer, G., Manning, G., and Malumbres, M. (2011) From Plk1 to Plk5: functional evolution of polo-like kinases. *Cell Cycle* **10**, 2255–2262
59. Attner, M. A., Miller, M. P., Ee, L. S., Elkin, S. K., and Amon, A. (2013) Polo kinase Cdc5 is a central regulator of meiosis I. *Proc. Natl. Acad. Sci. U.S.A.* **110**, 14278–14283